Supplementary Materials for

"Long-Range Charge Transfer and Oxygen Vacancy Interactions in Strontium Ferrite"

Tridip Das, Jason D. Nicholas, and Yue Qi

Chemical Engineering & Materials Science Department, Michigan State University, 428 South Shaw Lane, 2527 Engineering Building, East Lansing, MI 48824, USA

S1: Selection of U-parameter Based on Experimental Magnetic Moment and Lattice Parameters

The vacancy formation energy does depend on the selection of U parameter.[1] In this paper, the U parameter was selected based on the comparison with experimental lattice parameter and magnetic moment on Fe. In this study, GGA+U calculation with the U-parameter over the range of 0.2 to 4.0 were performed for both ferromagnetic (FM) $LaFeO_3$ and $SrFeO_3$ bulk structures. The computed magnetic moment and lattice parameters were compared with the experimental values as shown in Figure S1. The calculated magnetic moment on Fe in $SrFeO_3$ shows a steady increase with increasing U parameter but the magnetic moment on Fe in $LaFeO_3$ fluctuated, possibly due to the existence of additional minima due to different possible electronic distributions.[2] Reehuis *et al.*[3] have measured the magnetic moment of Fe in $SrFeO_3$ structure (without oxygen vacancy) with neutron diffraction at 2K and determined $\mu_{Fe^{4+}}$ = 2.96 μ_B. The experimental magnetic moment for Fe in $LaFeO_3$ reported by Koehler *et al.*[4] is $\mu_{Fe^{3+}}$ = 4.6 ± 0.2 μ_B. In this calculation, U_{eff} = 3 has led to the magnetic moment on Fe about 3.61 μ_B in $SrFeO_3$ and 4.23 μ_B in $LaFeO_3$, reasonably agreeing with both experimental values. Meanwhile U_{eff} = 3 has led to a good agreement between the predicted and measured[5,6] lattice parameters for both with $SrFeO_3$ and $LaFeO_3$ (with a maximum deviation of 1.75 %).

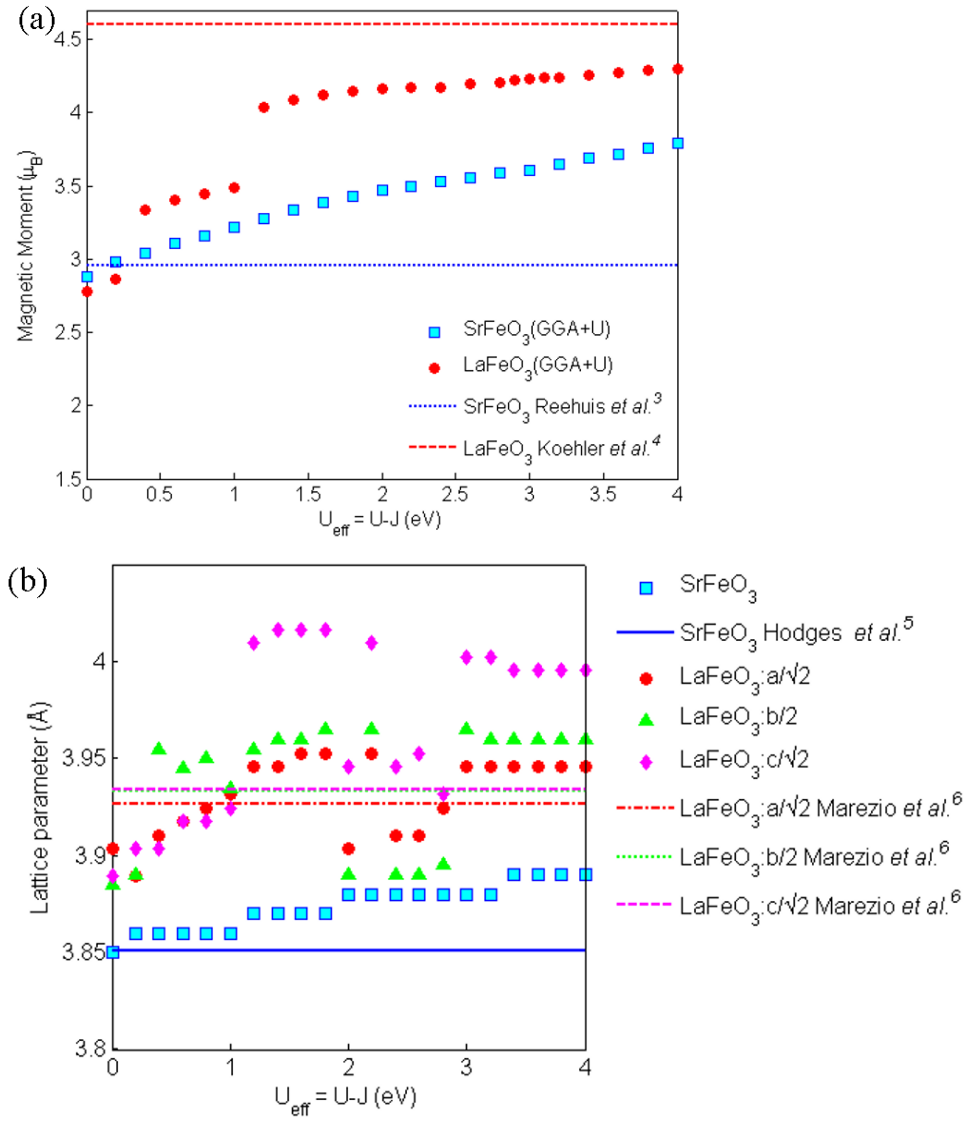

Figure S1 Plot of (a) magnetic moment and (b) lattice parameters as a function of U_{eff} parameter. The straight lines are experimental data, and blue and red correspond to the data for $SrFeO_3$ and $LaFeO_3$, respectively. Since $LaFeO_3$ is not cubic, red, green and pink colors in (b) are corresponding to reduced-scale lattice (a/√2, b/2, c/√2 respectively) of $LaFeO_3$.

S2: Derivation of Equation 5 from Chemical Potential of Oxygen Molecule

Assuming the oxygen atom in the lattice site is in chemical equilibrium with the gas phase oxygen molecule we can write Equation S1.

$$\mu_O(T,p) = \frac{1}{2}\mu_{O_2}(T,p) = \frac{1}{2}E_{O_2}^{DFT} + \frac{1}{2}\Delta\mu_{O_2}(T,p) \qquad [S1]$$

where $\Delta\mu_{O_2}(T,p)$ is the thermodynamic connection energy between DFT (0 K) calculated energy of an isolated oxygen molecule with free energy of oxygen molecule at any temperature, T and partial pressure, p. Equation S2 brakes $\Delta\mu_{O_2}(T,p)$ into three parts. The first part, $\Delta H_{O_2}|_{0K}^{T}$ is the enthalpy of connection energy. All the enthalpy related terms in this derivation are highlighted in red color. The second part, $T\Delta S_{O_2}|_{0K}^{T}$ is related to entropy correction. All the entropy related terms are highlighted in green color. The third part, $kTln\left(\frac{p}{p_0}\right)$ is the pressure correction term and highlighted in blue color.

$$\Delta\mu_{O_2}(T,p) = \Delta H_{O_2}|_{0K}^{T} - T\Delta S_{O_2}|_{0K}^{T} + kTln\left(\frac{p}{p_0}\right) \quad [S2]$$

Equation S3 substitutes the enthalpy and entropy related terms into their integral form.

$$\Delta\mu_{O_2}(T,p_0) = \int_{0K}^{T} C_p dT - T\int_{0K}^{T} \frac{C_p}{T} dT \quad [S3]$$

The enthalpy contribution to the connection energy is obtained by integrating the heat capacity, Cp over the temperature range 0 K to T (Equation S3) and it is separated into two parts as shown in Equation S4 for the ease of calculation. Similarly, the entropy term of the connection energy was also calculated in two parts as shown in Equation S5.

$$\Delta\mu_{O_2}(T,p_0) = \Delta h_{O_2}|_{0K}^{T_r=298K} + \int_{T_r=298K}^{T} C_p dT - T\int_{0K}^{T} \frac{C_p}{T} dT \quad [S4]$$

Here, $\Delta h_{O_2}|_{0K}^{T_r=298K}$ is the connection enthalpy for oxygen molecule between 0 K and standard state (298 K) which can be obtained in multiple ways as explained in next section.

$$\Delta\mu_{O_2}(T,p_0) = \Delta h_{O_2}|_{0K}^{T_r=298K} + \int_{T_r=298K}^{T} C_p dT - T\int_{0K}^{T_r=298K} \frac{C_p}{T} dT - T\int_{T_r=298K}^{T} \frac{C_p}{T} dT \quad [S5]$$

Rearrange the terms in Equation S5, it becomes

$$\Delta\mu_{O_2}(T,p) = \Delta h_{O_2}|_{0K}^{T_r=298K} - T\int_{0K}^{T_r=298K}\frac{C_p}{T}dT + \int_{T_r=298K}^{T} C_p dT - T\int_{T_r=298K}^{T}\frac{C_p}{T}dT + kTln\left(\frac{p}{p_0}\right) \quad [S6]$$

Subtracting and adding $T_r\int_{0K}^{T_r=298K}\frac{C_p}{T}dT$ in Equation S6 helps us to relate terms with chemical potential of oxygen, as shown in later steps.

$$\Delta\mu_{O_2}(T,p) = \Delta h_{O_2}|_{0K}^{T_r=298K} - T_r\int_{0K}^{T_r=298K}\frac{C_p}{T}dT - (T-T_r)\int_{0K}^{T_r=298K}\frac{C_p}{T}dT + \int_{T_r=298K}^{T} C_p dT - T\int_{T_r=298K}^{T}\frac{C_p}{T}dT + kTln\left(\frac{p}{p_0}\right) \quad [S7]$$

Now, $\int_{0K}^{T_r=298K}\frac{C_p}{T}dT$ is the standard entropy and can be obtained from thermodynamic handbook data and represented as S_r in Equation S8.

$$\Delta\mu_{O_2}(T,p) = \Delta h_{O_2}|_{0K}^{T_r=298K} - T_r\int_{0K}^{T_r=298K}\frac{C_p}{T}dT - (T-T_r)\,S_r + \int_{T_r=298K}^{T} C_p dT - T\int_{T_r=298K}^{T}\frac{C_p}{T}dT + kTln\left(\frac{p}{p_0}\right) \quad [S8]$$

$$\Delta\mu_{O_2}(T,p) = \Delta h_{O_2}|_{0K}^{T_r=298K} - T_r\int_{0K}^{T_r=298K}\frac{C_p}{T}dT + \int_{T_r=298K}^{T} C_p dT - T\int_{T_r=298K}^{T}\frac{C_p}{T}dT - (T-T_r)\,S_r + kTln\left(\frac{p}{p_0}\right) \quad [S9]$$

Defining the enthalpy and entropy of connection between 0 K and 298 K $\left(\Delta h_{O_2}|_{0K}^{T_r=298K} - T_r\int_{0K}^{T_r=298K}\frac{C_p}{T}dT\right)$ to be the change in chemical potential of oxygen $\Delta\mu_{O_2}^0(T_r)$ between 0 K and standard state, leads to:

$$\Delta\mu_{O_2}^0(T) = \Delta\mu_{O_2}^0(T_r) + \int_{T_r=298K}^{T} C_p dT - T\int_{T_r=298K}^{T}\frac{C_p}{T}dT - (T-T_r)\,S_r \quad [S10]$$

S3: Numerical Method to Find Temperature Corresponding to an Oxygen Nonstoichiometry for Certain O_2 Partial Pressure (MATLAB code) to Solve Equation 7.

```
% Temperature from nonstoichiometry
TC = 0:0.1:2000; % Temperature range in deg C
T = TC+273.15; % T in K
p = 0.21; % atm
R = 8.314e-3; % kJ/mol-K
cF = 96.485; % 1eV = 96.485 kJ/mol --> conversion Factor
Nv = 3; % # of available sites/ formula unit
x = 0.0625; % Nonstoichiometry
Evac_DFT = 0.56; % Vacancy formation energy
%
for i = 1:length(T)
    mu_O2_corr = O2_correction(T(i),p)/cF;
   %
    G_vac(i) = Evac_DFT + 0.5 * mu_O2_corr;
   %
    A_fac = exp(-G_vac(i)*cF/(R*T(i)));
    nonstoi(i) = Nv*A_fac/(1+A_fac);
%
    if nonstoi(i) >= x
       vac_form = E_vac(i);
       TempK=T(i);
       delta = nonstoi(i);
      break;
    end
end
%
TempC = TempK-273.15% Temperature in deg C
```

Function: O2_correction

```
function mu_O2_corr = O2_correction(T,p)
% This function returns connection energy in eV for oxygen MOLECULE
% between room temperature(298.15K) at 1 bar (0.987 atm) and
% any other temperature (K) and pressure (atm)
%
 Tr = 298.15; % K
 Sr = 205.152e-3; % kJ/mol-K
 p0 = 0.986923267; % atm
 R = 8.314e-3; % kJ/mol-K
 cF = 96.485; % 1eV = 96.485 kJ/mol --> conversion Factor
%
 delG_O2 = -0.28*2; % Ref # 123 Average for O2
%
     if T < 700
       % for Temp range 100 to 700 K
       A = 31.32234; % J/(mol-K) ******
http://webbook.nist.gov/cgi/cbook.cgi?ID=C7782447&Units=SI&Mask=1#Thermo-Gas *******
       B = -20.23531; % J/(mol-K^2)
       C = 57.86644; % J/(mol-K^3)
       D = -36.50624; % J/(mol-K^4)
       E = -0.007374; % J-K/mol
       F = -8.903471; % kJ/mol
       G = 246.7945; % J/(mol-K)
     else
```

```
        % for Temp range 700 to 2000 K
        A = 30.03235; % J/(mol-K) ******
http://webbook.nist.gov/cgi/cbook.cgi?ID=C7782447&Units=SI&Mask=1#Thermo-Gas *******
        B = 8.772972; % J/(mol-K^2)
        C = -3.988133; % J/(mol-K^3)
        D = 0.788313; % J/(mol-K^4)
        E = -0.741599; % J-K/mol
        F = -11.32468; % kJ/mol
        G = 236.1663; % J/(mol-K)
      end
%
 t = T/1000; % T in K
% del_H = H(pr,T) - H(pr,Tr)
 del_H = A*t +(B/2)*t^2 +(C/3)*t^3 +(D/4)*t^4 -E/t+F; % kJ/mol
%
% del_S = S(pr,T) - S(pr,Tr)
 S = A*log(t) +B*t +(C/2)*t^2 +(D/3)*t^3-E/(2*t^2)+G; % J/mol-K
 S = S/1000; % kJ/mol-K
 del_S = S - Sr;
%
 mu_O2_corr = delG_O2*cF + del_H - T*del_S - (T-Tr)*Sr + R*T*log(p/p0);  % as p0 = 1
bar
end
```

With this solution, we compare the oxygen vacancy concentration computed from Equation 6 (dotted line) and 7 (solid line), with and without an account of varying oxygen vacancy formation energy with concentrations.

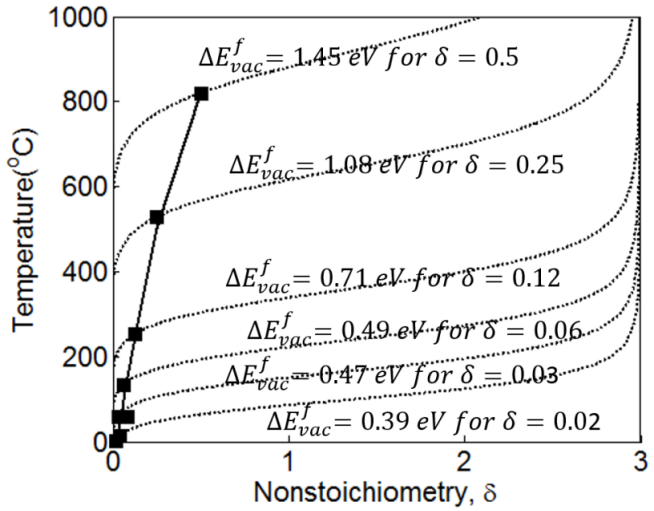

Figure S2. Dotted line represent δ increasing with T at pO_2 = 0.21 atm according to Equation 6 (dilute vacancy assumption) for cubic $SrFeO_{3-\delta}$ (ΔE^f_{vac} from Figure 4 for different δ). Solid line represent δ increasing with T at atmospheric condition according to Equation 7 (interacting vacancy assumption) for cubic $SrFeO_{3-\delta}$ (where ΔE^f_{vac} is a function of δ)

S4: Computationally Predicted Phase stability in $SrFeO_{3-\delta}$ Phases

It is known that DFT+U calculation does a poor job in predicting phase transition in materials, especially when metal to insulator phase transition happens but our selection of U parameter in this study was able to capture the energetically favored phases when oxygen vacancy ordered phase transitions occurred at a certain oxygen non-stoichiometry. In order to determine energetically favorable arrangements, the excess energy (ΔE^{δ}) of various oxygen deficient structures (cubic, tetragonal, orthorhombic, and brownmillerite) with respect to the perfect cubic $SrFeO_3$ was defined and compared via the relation:

$$\Delta E^{\delta} = E^{DFT}_{SrFeO_{3-\delta}} + \frac{\delta}{2} E^{DFT}_{O_2} - E^{DFT}_{SrFeO_3} \quad [S11]$$

where $E^{DFT}_{SrFeO_{3-\delta}}$ is the energy of the oxygen deficient arrangement of interest, $E^{DFT}_{O_2}$ is the energy of an isolated oxygen molecule, and $E^{DFT}_{SrFeO_3}$ is the energy of the perfect cubic $SrFeO_3$.

Experimentally, with increasing T and the increasing δ accompanying it, strontium ferrite displays several phase transitions as it progresses from cubic $SrFeO_3$ to tetragonal $SrFeO_{2.875}$ (with δ^0=0.125), to orthorhombic $SrFeO_{2.75}$ (with δ^0=0.25), and finally to brownmillerite $SrFeO_{2.5}$ (with δ^0=0.5). However, it has not been clear if these phase changes are induced by T or by δ. Thankfully, DFT calculations such as those in Figure S3 where the *X* for any structure can be arbitrarily increased as long as δ is $> \delta^o$ for the structure of interest (including those not observed in nature because of a phase transformation to a lower energy crystal structure) allow the effects of oxygen non-stoichiometry alone to be examined. Specifically, Figure S3 shows that at 0 K cubic strontium ferrite has the lowest energy from $0<\delta<0.125$, tetragonal strontium ferrite has the lowest energy from $0.125<\delta<0.25$, tetragonal and orthorhombic strontium ferrite have similar energies from $0.25<\delta<0.50$, and brownmillerite has the lowest energy for $\delta>0.50$. This suggests that oxygen non-stoichiometry instead of temperature is the dominant force driving the strontium ferrite phase transformations observed from 0-1400 ^{o}C in air. Further, these DFT

calculations indicate that the enthalpy gain in the cubic to tetragonal or orthorhombic to brownmillerite phase transitions are larger than the configurational entropy contributions.

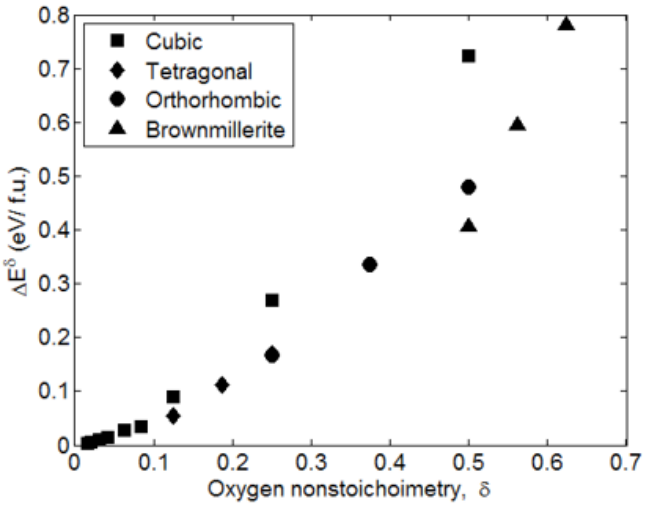

Figure S3. Energy required $\left(\Delta E^{\delta}\right)$ to form the non-stoichiometric structures $\left(SrFeO_{3-\delta} + \frac{\delta}{2}O_2\right)$ from cubic $SrFeO_3$

References for the Supplemental materials.

(1) Kuklja, M. M.; Kotomin, E. A.; Merkle, R.; Mastrikov, Y. A.; Maier, J. Combined Theoretical and Experimental Analysis of Processes Determining Cathode Performance in Solid Oxide Fuel Cells. *Phys. Chem. Chem. Phys.* **2013**, *15* (15), 5443.
(2) Gryaznov, D.; Heifets, E.; Kotomin, E. The First-Principles Treatment of the Electron-Correlation and Spin–orbital Effects in Uranium Mononitride Nuclear Fuels. *Phys. Chem. Chem. Phys.* **2012**, *14* (13), 4482–4490.
(3) Reehuis, M.; Ulrich, C.; Maljuk, A.; Niedermayer, C.; Ouladdiaf, B.; Hoser, A.; Hofmann, T.; Keimer, B. Neutron Diffraction Study of Spin and Charge Ordering in SrFeO3−δ. *Phys. Rev. B* **2012**, *85* (18), 184109.
(4) Koehler, W. C.; Wollan, E. O. Neutron-Diffraction Study of the Magnetic Properties of Perovskite-like Compounds LaBO3. *J. Phys. Chem. Solids* **1957**, *2* (2), 100–106.
(5) Hodges, J. P.; Short, S.; Jorgensen, J. D.; Xiong, X.; Dabrowski, B.; Mini, S. M.; Kimball, C. W. Evolution of Oxygen-Vacancy Ordered Crystal Structures in the Perovskite Series SrnFenO3n−1 (n=2, 4, 8, and ∞), and the Relationship to Electronic and Magnetic Properties. *J. Solid State Chem.* **2000**, *151* (2), 190–209.
(6) Marezio, M.; Dernier, P. D. The Bond Lengths in LaFeO3. *Mater. Res. Bull.* **1971**, *6* (1), 23–29.